RESEARCH ARTICLE

Correspondence to:
Z.-H. Tan,
tanzh@xtbg.ac.cn

Interannual and seasonal variability of water use efficiency in a tropical rainforest: Results from a 9 year eddy flux time series

Zheng-Hong Tan[1], Yi-Ping Zhang[1], Xiao-Bao Deng[1], Qing-Hai Song[1], Wen-Jie Liu[1], Yun Deng[1], Jian-Wei Tang[1], Zhi-Yong Liao[1], Jun-Fu Zhao[1], Liang Song[1], and Lian-Yan Yang[1]

[1]Key Laboratory of Tropical Forest Ecology, Xishuangbanna Tropical Botanical Garden, Chinese Academy of Sciences, Kunming, China

Abstract We used a continuous 9 year (2003–2011) eddy flux time series with 30 min resolution to examine water use efficiency in a tropical rainforest and determine its environmental controls. The multiyear mean water use efficiency (W_{ue}) of this rainforest was 3.16 ± 0.33 gC per kg H_2O, which is close to that of boreal forests, but higher than subtropical forests, and lower than temperate forests. The water vapor deficit (V_{PD}) had a strong impact on instantaneous W_{ue}, in the manner predicted by stomatal optimization theory. At the seasonal scale, temperature was the dominant controller of W_{ue}. The negative correlation between temperature and W_{ue} was probably caused by high continuous photosynthesis during low-temperature periods. The V_{PD} did not correlate with W_{ue} at the interannual scale. No interannual trend was detected in W_{ue} or inherent water use efficiency (W_{ei}), either annually or seasonally. The fact that no increasing trend of W_{ei} was found in the studied tropical rainforest, along with other evidence of CO_2 stimulation in tropical rainforests, requires special attention and data validation. There was no significant difference between W_{ue} during a drought and the 9 year mean values in the forest we studied, but we found that dry season transpiration (T_r) was consistently lower during the drought compared to the mean values. Finally, whether W_{ue} increases or decreases during a drought is determined by the drought sensitivity of gross primary production (G_{PP}).

1. Introduction

Plants assimilate carbon from and transpire water to the atmosphere [*Mencuccini et al.*, 2004]. The water loss and carbon gain are two processes coupled through stomata [*Hsiao and Acevedo*, 1974]. The concept of water use efficiency (W_{ue}) was introduced to describe these coupled processes [*deWit*, 1958], and the term is widely used in agricultural and arid ecosystems studies [*Sinclair et al.*, 1983]. Based on the idea of conductance, *Bierhuizen and Slatyer* [1965] gave W_{ue} a solid physiological basis, which was enforced later by *Cowan and Farquhar* [1977] by examining stomata function.

In view of W_{ue} studies in recent years, there are several issues that still have not been well addressed, as follows.

1. *Ecosystem-level W_{ue} studies*. Before the 2000s, most studies on W_{ue} were concentrated at leaf level [*Morén et al.*, 2001; *Law et al.*, 2002; *Ponton et al.*, 2006]. Ecosystem-level knowledge of carbon and water trade-off is the basis for global change studies, not only because carbon and water exchange are important land surface processes which directly affect atmospheric circulation but also because water is an important limiting factor on vegetation metabolism, production, and distribution. Furthermore, W_{ue} could be used to estimate the large-scale carbon budget [*Beer et al.*, 2007] and is thus very important, especially for addressing the unsolved missing carbon sink problem [*Pan et al.*, 2011].
2. *Long-term W_{ue} and its environmental controls*. Most long-term (i.e., decadal) records of W_{ue} have been inferred from tree ring isotopes [*Peñuelas et al.*, 2011; *Nock et al.*, 2011]. The only study using direct long-term W_{ue} records was aimed at addressing CO_2 fertilization [*Keenan et al.*, 2013]. How other environmental factors control long-term W_{ue} have not been fully discussed.
3. *Forest ecosystem W_{ue}*. Forest ecosystem W_{ue} has been less studied compared to crops and grasslands. This is not only because of the high practical value of agricultural production but also because of the lack of proper methods to directly measure whole ecosystem W_{ue} [*Morén et al.*, 2001]. As forests comprise a large part of land coverage, good knowledge of forest ecosystem W_{ue} is necessary for both global change studies and forest management.

4. *V_{PD} effect on W_{ue}*. Water vapor pressure deficit (V_{PD}) has a strong effect on W_{ue} [*Bierhuizen and Slatyer*, 1965; *Lange et al.*, 1971]. Instantaneous water use efficiency depends on V_{PD}, as predicted by stomatal optimization theory, as $1/(V_{PD})^{0.5}$ [*Katul et al.*, 2009]. This was confirmed by observation data from an oak forest [*Yang et al.*, 2010]. Nevertheless, how V_{PD} controls seasonal and interannual W_{ue} has not been well examined.

5. *Effect of severe drought on W_{ue}*. Ecosystem water use efficiency reportedly decreased during the 2003 European heat wave, which coincided with a severe drought [*Reichstein et al.*, 2007]. However, the reduction of W_{ue} was slight. In contrast, water use efficiency of Swiss forests increased during a spring drought, which resulted in reduction of evapotranspiration [*Wolf et al.*, 2013]. The two cases reviewed here are from quite different bioclimate regimes. This may be the main reason behind the difference in W_{ue} changes between them. Tree ring isotope studies suggested that low water availability would reduce the W_{ue} rate, while the increasing W_{ue} was caused by CO_2 fertilization [*Linares and Camarero*, 2012]. *Yang et al*. [2010] found that stomata optimization will break down in severe drought and exert an impact on W_{ue}. Considering its unique climate seasonality and functional types, tropical rainforest is expected to have different patterns of W_{ue} change.

The eddy covariance method can provide ecosystem-level direct measurements of water vapor and carbon dioxide fluxes [*Goulden et al.*, 1996; *Law et al.*, 2002] and is a popular method in ecosystem studies. In China, for example, it was estimated that more than 200 eddy flux sites exist [*Xiao et al.*, 2013]. Several synthetic studies have used these large data sets to address ecosystem water use efficiency. *Beer et al*. [2009], for example, investigated the variability of inherent water use efficiency (W_{ei}) among different sites. *Keenan et al*. [2013] tested the CO_2 fertilization hypothesis with long-term forest W_{ei} records. *Yu et al*. [2008] addressed the water use efficiency of China's forests and its environmental controls. However, no tropical rainforest ecosystems were included in these studies. Several questions concerning tropical rainforest water use efficiency still need to be answered, such as the following. What is the magnitude of tropical rainforest water use efficiency? Is it higher than temperate and boreal forests? What are the daily, seasonal, and interannual patterns of tropical forest water use efficiency? How do environmental factors control water use efficiency? How does tropical rainforest water use efficiency respond to severe drought? In this study, we use 9 year continuous eddy flux data collected from a Chinese tropical rainforest to address these questions.

2. Methods

2.1. Site Description

Land cover in China includes continuous forest biomes, from boreal, temperate, and subtropical forests, as well as tropical forests at the southern edge. Generally, tropical forests in China occur mainly on Hainan Island (land area: 354,000 km^2) and Xishuangbanna Prefecture (19,500 km^2). The tropical forest of Xishuangbanna Prefecture is an extension of tropical Southeast Asia [*Zhu and Yan*, 2009]. Compared to the lowland rainforests near the equator, Xishuangbanna's rainforests exist in a more seasonal climate.

Our study site is located in Menglun Town, Mengla County, Xishuangbanna Prefecture, Yunnan Province of Southwest China (101°15′E, 21°55′N) (Figure 1). The site is a long-term ecological research site established around 1992–1993 by pioneer tropical ecologists. Typical research facilities include forest catchments, micrometeorological towers, and dynamic permanent plots. The micrometeorological tower used in this study was established in 1994–1995. The tower is made of iron in a triangular shape and is 70 m tall.

As mentioned before, the climate is strongly seasonal. According to climatic observation at a meteorological station in the past half century (1959–2008), the mean annual temperature is 21.8°C, and the mean annual rainfall is 1511 mm. Over 85% of the annual rainfall occurs in the rainy season (May through October). Mean monthly rainfall during the dry season is less than 40 mm.

The soil is lateritic, derived from siliceous rocks such as granite and gneiss, with a pH of 4.5–5.5. The forest canopy is uneven and complex and can be divided into three layers. The leaf area index (L_{AI}) varies from 4.0 to 6.0 throughout the year (based on LAI-2000 observations). Trees in the topmost layer (>30 m in height) primarily include *Pometia tomentosa*, *Terminalia myriocarpa*, *Gironniera subaequalis*, and *Garuga floribunda*, with an average canopy height of 30–35 m. The second layer is 16–30 m in height, composed of *Barringtonia*

Figure 1. The geographic location of the study site (star).

macrostachya, *Gironniera subaequalis*, and *Mitrephora maingayi*. The lowest layer (<16 m) includes trees, shrubs, and seedlings. Frequently occurring tree species are *Garcinia cowal*, *Knema erratica*, *Ardisia tenera*, *Mezzettiopsis creaghii*, *Dichmpetalum gelonioides*, *Saprosma ternatum*, and *Morinda angustifolia*.

2.2. Eddy Covariance Observations

The eddy covariance technique is based on atmospheric turbulence and micrometeorology [*Baldocchi et al.*, 1988]. It is a popular method for studying ecosystem processes, and many eddy covariance sites have been established in the past two or three decades. In China, for example, it is estimated that more than 200 eddy flux sites existed in 2010 [*Xiao et al.*, 2013]. If we consider a period of time long enough to allow the passage of many eddies, some moving up, some moving down, the average rate at which scalars (i.e., water, CO_2, and heat) are transferred upward/downward at those points is the following [*Swinbank*, 1951]:

$$F = n^{-1} \sum \rho ws = \overline{\rho ws} \tag{1}$$

where F is flux, n is the number of observations, ρ is air density, w is vertical wind velocity, s is the target scalar, and the overbar indicates averaging. After Reynolds decomposition, and supposing that the air density fluctuations are negligible and the mean vertical flow is zero, we obtain F [*Burba*, 2013]:

$$F == \rho \overline{w's'} \tag{2}$$

where the primes represent fluctuations from the average.

In particular, the storage flux of carbon will become significant in tall tropical forest canopies. When estimating carbon fluxes, the storage flux term was included and calculated following *Hollinger et al.* [1994]

$$F_c = \rho \overline{w'c'} + \frac{dc}{dt} z_r \tag{3}$$

where c is CO_2 concentration measured by an infrared gas analyzer (Model Li-7500, Li-Cor Inc., USA), dc/dt is the change in CO_2 concentration with time, and z_r is the measurement height (48.8 m).

It has been suggested that the eddy covariance sensor is best mounted at 1.5 times the mean canopy height. In our tower, the sensor height was 48.8 m. Wind velocity was monitored by a 3-D sonic anemometer (CSAT-3, Campbell Scientific Inc., USA) and expressed in Cartesian coordinates. Density of CO_2 and water vapor was measured by an open-path infrared gas analyzer (Li-7500, Li-Cor Inc., USA). Data retrieval was conducted at a frequency of 10 Hz by a controller (data logger model CR5000, Campbell Scientific Inc., USA) and sent to a desktop computer placed in a nearby small house.

2.3. Microclimatic Observations

Microclimatic factors were measured as companions to the eddy covariance data. These factors were radiation, temperature, humidity, mean wind speed, photosynthetic active radiation, precipitation, soil temperature, heat flux, and water content. All data were recorded every 30 min to match the eddy flux. The rain gauge at the top of the tower was frequently blocked by ant nests. We therefore used rainfall data from a nearby standard meteorological station (3 km away) to replace the tower measurements.

Microclimatic instruments related to this study included a solar radiometer (CM11, Kipp & Zonen, the Netherlands) and rain gauge (52203, RM Young, USA) mounted at the top of the tower (70 m). Air temperature

and humidity were monitored by a hydrothermograph (HMP45C, Vaisala, Finland). Photosynthetic active radiation sensors (LI-190SB, Li-Cor. Inc., USA) were placed at heights of 3.9, 10.2, 21.0, 31.2, and 36.2 m. Soil water content was measured with time domain reflectometers (CS616, Campbell Scientific Inc., Logan, UT, USA) at depths of 5, 20, and 40 cm.

2.4. Data Processing, Calculations, and Statistics

Fluxes were calculated with a mean average period of 30 min. We set limits to exclude hard spikes in the fluxes. The upper and lower limits for carbon water and latent heat flux were 3 and -3 mg CO_2 m^{-2} s^{-1}, and -300 and 1000 w m^{-2}, respectively. Photosynthesis assimilation stopped at nighttime. Eddy fluxes observed at night were mainly contributed by ecosystem respiration (R_e). Assuming this principle, we estimate the gross primary production (an index describing total photosynthesis assimilation at the ecosystem level) to be

$$G_{PP} = -(F_c - R_e) \tag{4}$$

where the minus sign outside the parentheses is due to the discipline convention. R_e is the sum of nighttime and daytime R_e. Conceptually, nighttime carbon flux (F_c) equals nighttime R_e. However, nighttime F_c was usually underestimated during low wind speed periods when turbulence was not well developed. This is a common situation for nighttime observations at tropical rainforest sites. The common way to correct this underestimation is the so-called $u*$ filtering method ($u*$ is friction velocity) [*Goulden et al.*, 1996]. In this method, the threshold $u*$ was determined by finding a saturation point in a $u*$ and nighttime flux plot [*Reichstein et al.*, 2005]. All values less than the $u*$ threshold will be removed. We applied the $u*$ filtering to our data set. The post $u*$ filtering nighttime R_e was used to extrapolate the daytime R_e. We first related the nighttime R_e to temperature using *Lloyd and Taylor's* [1994] equation,

$$R_{e,nightime} = R_{ref} \exp\left(E_0 \left(\frac{1}{T_{ref} - T_0} - \frac{1}{T - T_0} \right) \right) \tag{5}$$

where $R_{e,nightime}$ is nighttime R_e, R_{ref}, E_0, and T_0 are fitted parameters, T_{ref} is the reference temperature (here 20°C), and T is the nighttime measured temperature. The relationship between nighttime R_e and temperature is significant at annual scales, with daily mean values ($r^2 > 0.5$, $p < 0.01$) [*Tan et al.*, 2009]. Then, daytime R_e was extrapolated using the specific regression and measured temperature.

Data gaps generated by bad weather (i.e., heavy rainfall), power failure, hard spikes, and $u*$ filtering was filled by the regression method [*Falge et al.*, 2001; *Reichstein et al.*, 2005]. We did not process the data using a self-coded program but uploaded them to a commonly used online program to accomplish $u*$ filtering, gap filling, and flux partitioning (http://www.bgc-jena.mpg.de/~MDIwork/eddyproc/). Energy balance closure correction was not included for latent heat estimation [*Yu et al.*, 2008]. The energy balance closure is a site property and would not vary by much year to year. Thus, the energy balance closure correction should not affect the interannual trend of latent heat.

W_{ue} used in the study was defined as

$$W_{ue} = \frac{G_{PP}}{T_r} \tag{6}$$

where T_r is canopy transpiration. In addition, we used W_{ei}, following *Beer et al.* [2009],

$$W_{ei} = W_{ue} \cdot V_{PD} = \frac{G_{PP} \cdot V_{PD}}{T_r} \tag{7}$$

where V_{PD} is water vapor pressure deficit. Since V_{PD} has a strong impact on W_{ue}, W_{ei} was suggested to be more appropriate for investigating the response of ecosystem water use efficiency to environmental variations [*Beer et al.*, 2009].

In order to obtain canopy transpiration (T_r), we first converted the eddy covariance recorded latent heat flux (L_E) into evapotranspiration (ET),

$$ET = \frac{L_E}{\lambda} \tag{8}$$

where λ is latent heat of vaporization. *ET* is the sum of transpiration from trees (T_r), evaporation from the forest floor, and evaporation from the wet canopy. Since our studied primary tropical rainforest has a
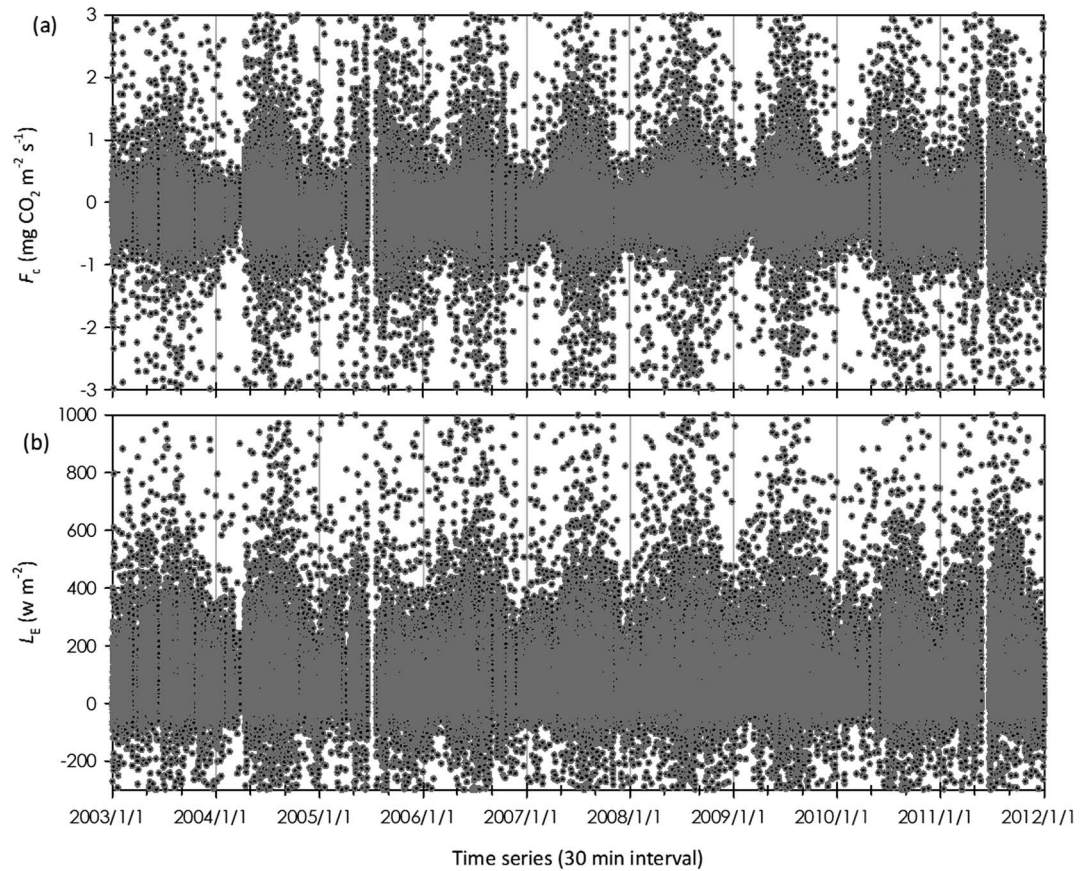
Figure 2. Raw time series of (a) carbon fluxes (F_C) and (b) latent heat flux (L_E) collected during 2003–2011 with 30 min resolution.

dense and fully closed canopy year-round, evaporation from the forest floor could be negligible. Finally, we excluded wet canopy values by omitting eight data points (4 h) during and after each rainfall event. Our work experience showed that 4 h is enough to turn a wet canopy into a dry canopy in the tropical forest.

We did not carry out additional corrections for advection problems, not only because we lack data to account for the unsolved advection term [*Aubinet et al.*, 2010] but also because our focus is mainly on daytime data, whereas most of the advection occurs during the night. Furthermore, we already perform $u*$ filtering on the nighttime data, which can partly avoid observations with significant advection terms involved in the flux estimation.

In addition, we calculated the L_{AI} and sky clearness index (k_t) to examine whether they can explain W_{ue}'s seasonality. L_{AI} is calculated from light transmittance (τ) as [*Baldocchi*, 1994]

$$L_{AI} = -\frac{1}{\kappa}\ln(\tau)\sin\beta = -\frac{1}{\kappa}\ln\left(\frac{Q_{tr}}{Q_i}\right)\sin\beta \tag{9}$$

where κ is the extinction coefficient, β is the solar elevation angle, Q_{tr} is the transmitted radiation (here it is the photosynthetic active radiation (PAR) measured at 3.9 m), and Q_i is incident radiation (PAR at 36.2 m). The value of k_t was calculated following *Gu et al.* [1999]:

$$k_t = \frac{S_i}{S_o} = \frac{S_i}{1368\times(1 + 0.033\cdot\cos(360\cdot DOY/365))\times\sin\beta} \tag{10}$$

where S_i is the measured incident solar radiation, S_o is the theoretical incident solar radiation, DOY is day of year, and k_t varies from 0 (cloudy) to 1 (clear). The interannual trend analysis was carried out using the Mann-Kendall test.
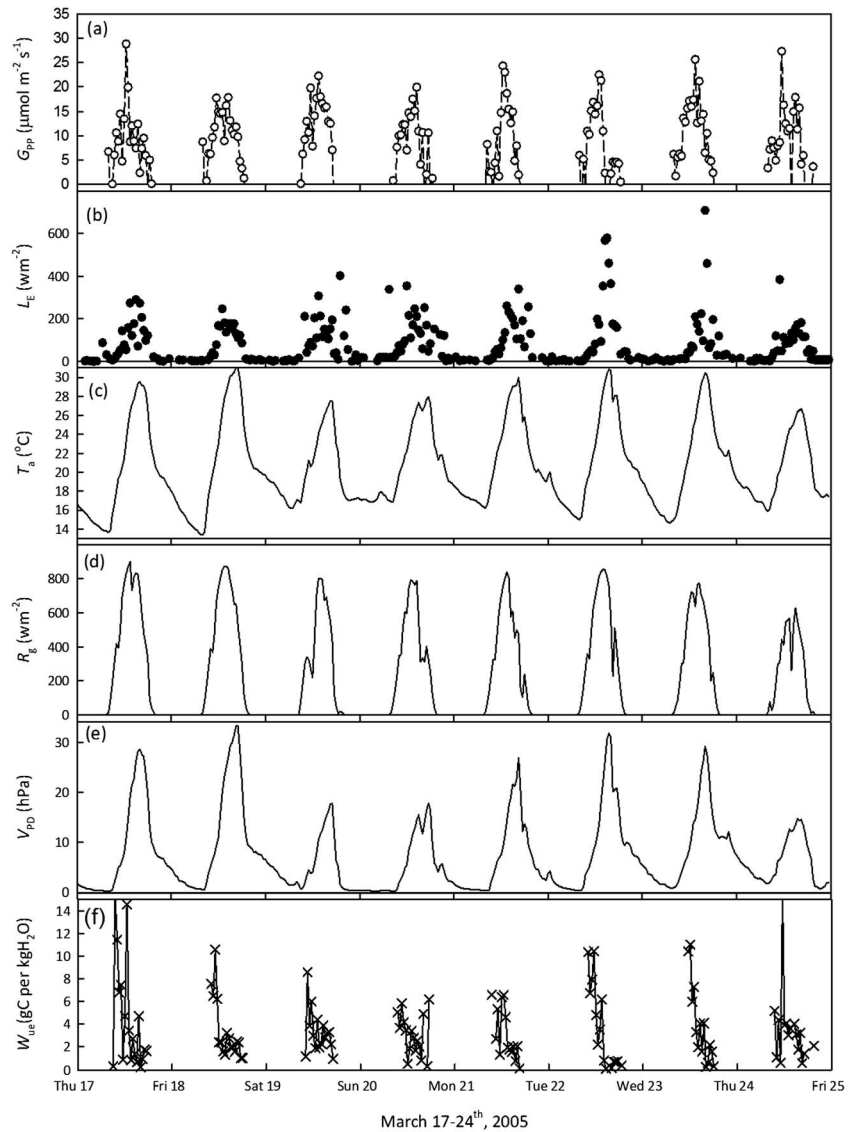
Figure 3. Eight days of data without rainfall collected during 17–24 March 2005. G_{PP}, L_E, T_a, R_g, V_{PD}, and W_{ue} represent gross primary production, latent heat flux, air temperature, solar radiation, water vapor pressure deficit, and water use efficiency, respectively.

3. Results

3.1. Raw Time Series of Carbon and Water Fluxes

Continuous 9 year (2003–2011) carbon and water fluxes were obtained, except for some short data gaps caused by instrument or power failures (Figure 2). Valid measurements of F_c and L_E were 137,854 and 137,843 half hours, or 87.37% and 87.36% of the time, respectively. A major challenge and source of uncertainty for long-term trend analysis is presented by the large data gaps contained in the time series. The continuous time series here is helpful for obtaining a defensible estimate of the interannual trend.

The upper and lower 95% percentiles of F_c are 0.738 and -0.791 mg CO_2 m^{-2} s^{-1} (Figure 2a), respectively. The median value is -0.034 mg CO_2 m^{-2} s^{-1}, indicating a moderate carbon sink. Both daytime negative values (net carbon uptake) and nighttime positive values (respiration carbon release) were higher during the rainy season (May through October) than during the dry season. The seasonality is stronger in the nighttime positive values than in the daytime negative values. This results in an unexpected F_c seasonal pattern: a carbon sink in the dry season and a carbon source in the rainy season [Zhang et al., 2010].
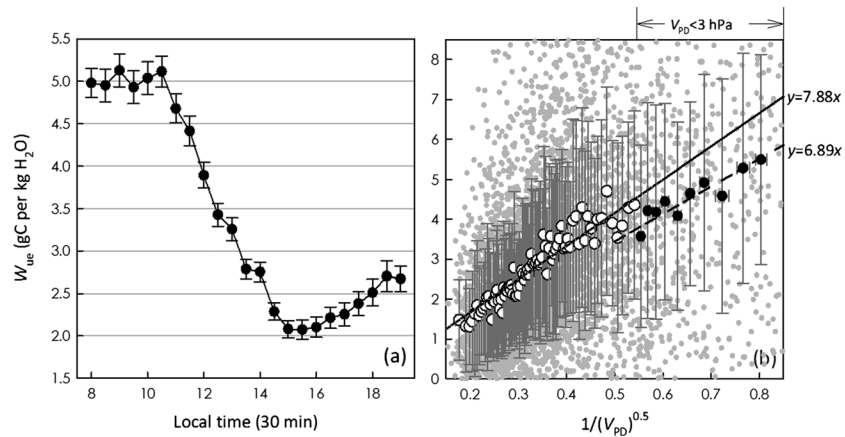
Figure 4. (a) The diurnal dynamic of water use efficiency (W_{ue}) and (b) response of W_{ue} to water vapor deficit (V_{PD}) with 30 min data. Grey circles are 30 min instantaneous measurements; they were binned into 100 parts with same number of data in each part (black solid and open circles). Error bars indicate standard deviations. Values with VPD < 3 hPa was marked with solid circles, and its regression line was in dashed style in Figure 4b.

The upper and lower 95% percentiles of L_E are −47 and 313 w m^{-2} (Figure 2b), respectively. The upper 95% percentile is smaller than but near the maximum value of the mean diurnal L_E during the rainy season (335 ± 136 w m^{-2}). Similar to F_c, L_E was higher during the rainy season than during the dry season. This seasonal pattern of L_E has been reported to be mainly controlled by L_{AI}, V_{PD}, and soil water content (S_{WC}) [Li et al., 2010].

3.2. Short Time Scale Variation of W_{ue} and Related Climatic Variables

Eight days (17–24 March 2005) of data were selected for short time scale analysis (Figure 3). No rainfall (rain gauge values larger than 0.1 mm per 30 min were treated as rainy days) occurred during this period, except on the last day. G_{PP} and L_E showed similar diurnal variations and are correlated ($r = 0.335$, $p < 0.01$, $n = 189$) (Figures 3a and 3b). Since W_{ue} was calculated as the ratio of G_{PP} and L_E, small variations in G_{PP} or L_E could lead to significant perturbations of the ratio. The diurnal pattern of W_{ue} was not as clear as expected (Figure 3f). Nevertheless, we generally found that W_{ue} was higher in the morning than in the afternoon, suggesting a nonsymmetrical pattern. Actually, W_{ue} varied strongly during the day, ranging from ~10 gC per kg H$_2$O in the morning to ~2 gC per kg H$_2$O in the late afternoon. At the short time scale, W_{ei} significantly correlated to and can partly be explained by V_{PD} ($r^2 = 0.2303$, $p < 0.01$) and temperature ($r^2 = 0.296$, $p < 0.01$).

Since 8 days observations are not statistically enough for obtain solid results and general pattern on short time scale, all 30 min data during 2003 were used to give a further analysis. Daytime W_{ue} varied strongly from 5.0 gC per kg H$_2$O in the early morning to 2.0 gC per kg H$_2$O in the afternoon and showed a clear diurnal pattern (Figure 4a). This is consistent with results in 8 days samples. We also related short time W_{ue} to V_{PD} in the manner predicted by stomatal optimization theory (Figure 4b). Generally, observations obey the rules prediction by stomatal optimization theory which indicated by a linear relationship between W_{ue} and $1/(V_{PD})^{0.5}$. We also noticed that the slope reduced under low V_{PD} (<3 hPa) (solid circles in Figure 4b).

3.3. The Annual Circle of W_{ue}, W_{ei}, and Related Biological or Climatic Variables

Some of the canopy trees shed their leaves in the late dry season (March and April, Figure 5e) to cope with the soil water deficit (Figure 5d) and high atmospheric water demand (Figure 5a). We anticipated a sudden decrease of W_{ue} during this period. Although W_{ue} was observed to be lowest in the late dry season (2.99 ± 0.37 gC per kg H$_2$O), the decrease of W_{ue} is moderate when compared to the rainy season (3.00 ± 0.28 gC per kg H$_2$O) and early dry season (3.50 ± 0.63 gC per kg H$_2$O) (Figure 5g).

W_{ue} is highest (up to 5 gC per kg H$_2$O) in DOY 1–30 and 330–365, during which the temperature is lowest (Figure 5g). At the annual scale, temperature (T_a) showed the highest significant correlation with W_{ei} (Figure 6a and Table 1). Although located in the tropical region, the annual temperature range (~10°C) is still largely higher than in the equatorial tropics (Figure 5c). The lowest temperature in December and
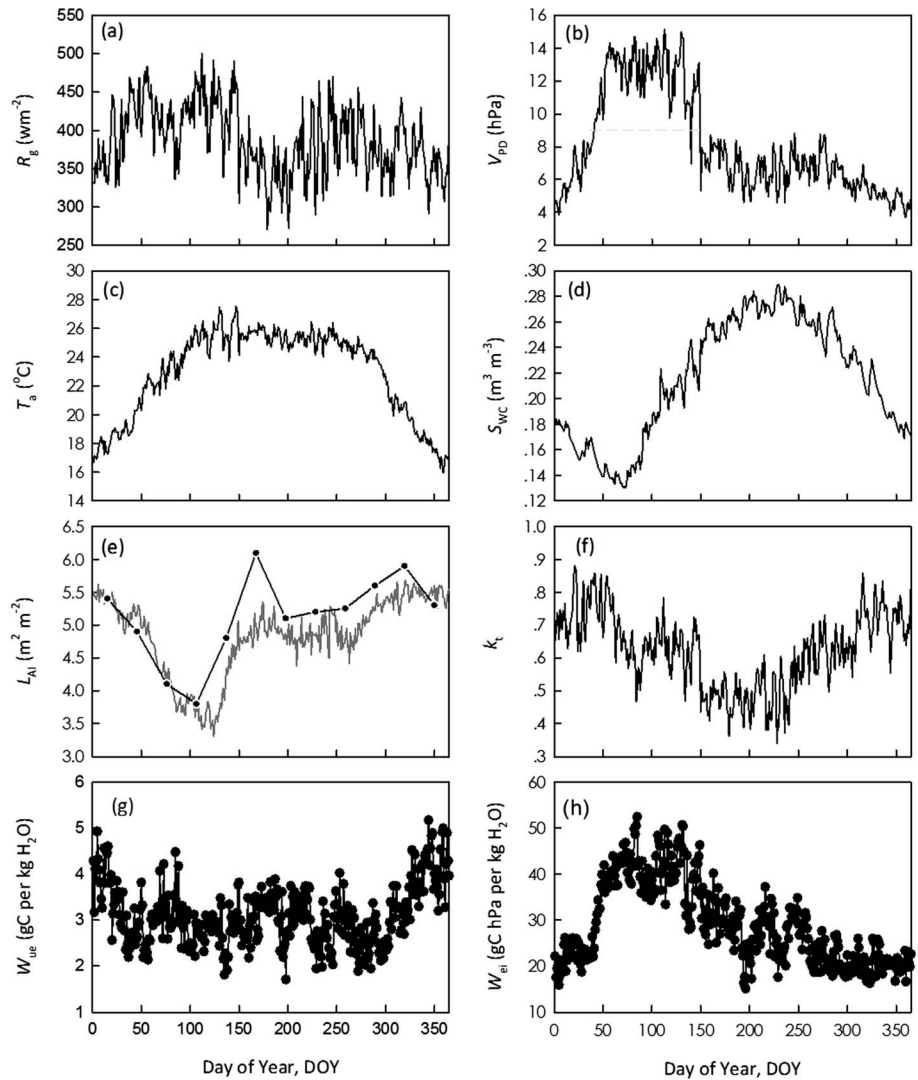
Figure 5. Annual circle of (a) solar radiation (R_g), (b) water vapor pressure deficit (V_{PD}), (c) air temperature (T_a), (d) soil water content (S_{WC}), (e) leaf area index (L_{AI}), (f) sky clearness index (k_t), (g) water use efficiency (W_{ue}), and (h) inherent water use efficiency (W_{ei}) with daily binned values. The solid circles connected by a black line in Figure 5e are L_{AI} observed with LAI-2000 [*Lin et al.*, 2011]; dark grey line indicates the daily value estimated from light transmittance.

January is around 17°C. Low temperature could lead directly to a decline in transpiration rate according to Penman-Monteith's principles [*Monteith*, 1964]. This decline would be strengthened when coinciding with lower solar radiation energy (Figure 5a). Meanwhile, the decrease of gross photosynthetic carbon assimilation (G_{PP}) was moderate and less than the degree of T_r. These could be explanations for the annual pattern of W_{ue} and its strong correlation with T_a.

W_{ei} and V_{PD} showed a similar pattern (Figures 5b and 5h) and are highly correlated (Figure 6b). This can easily be understood by considering the definition of W_{ei} ($W_{ei} = G_{PP}/T_r*V_{PD}$) and the extremely high V_{PD} in the late dry season. Besides V_{PD}, W_{ei} also highly correlated with L_{AI} (Figure 6c). This high-correlation relationship can be viewed as the indirect impact of V_{PD} on W_{ei}, since V_{PD} and L_{AI} were highly correlated with each other ($r = -0.78$, $p < 0.001$) and have a causal relationship [*Tan et al.*, 2014].

3.4. Interannual Trend of W_{ue} and W_{ei}

Annual mean W_{ue} varied from ~2.9 (2010) to 3.8 gC per kg H_2O (2005) (Figure 7a). The multiyear average W_{ue} was 3.16 ± 0.33 (mean ± standard deviation) gC per kg H_2O. The dry season, rainy season, and annual mean W_{ue} showed similar patterns. In general, W_{ue} during the dry season was higher than during the
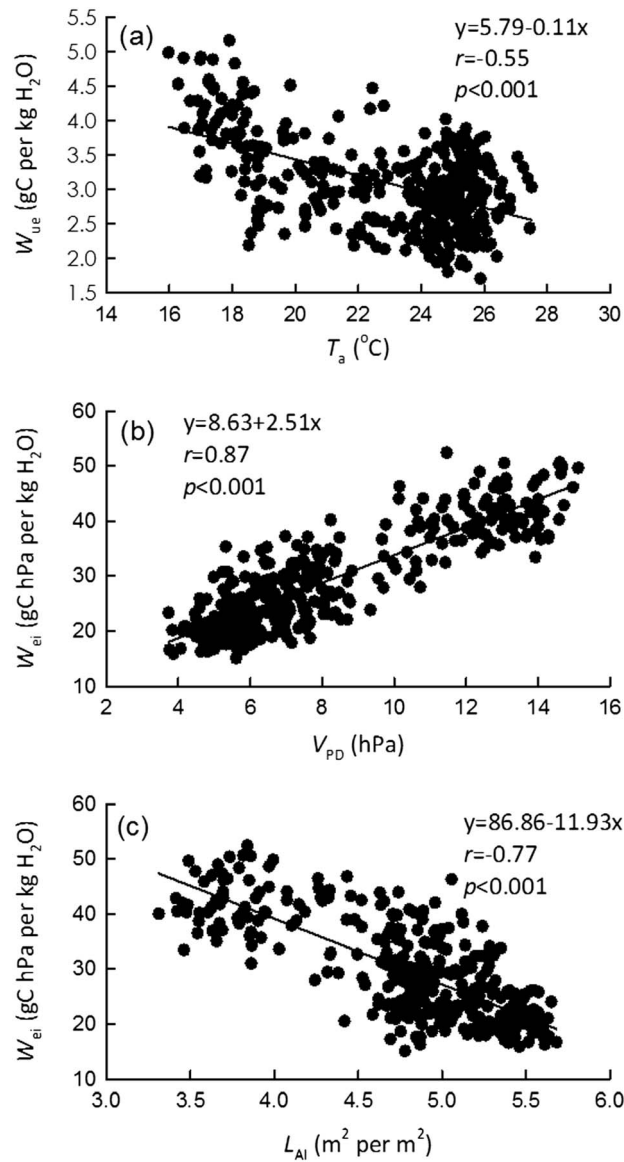
Figure 6. Environmental controls on annual variation of W_{ue}. (a) Air temperature, (b) water vapor pressure deficit, and (c) leaf area index. Linear regression (solid line) and regression results are also shown in the panel. The p value is two-tailed.

rainy season, except for in 2005. The interannual trend did not pass the Mann-Kendall trend test ($p = 0.23$), and neither did the seasonal and annual means.

The interannual variations of W_{ei} and W_{ue} were highly and significantly correlated ($r = 0.84$, $p < 0.01$), except for values in 2010. An interannual trend of W_{ei} was not detected in either the seasonal or annual mean values (Mann-Kendall test, $p > 0.70$). The multiyear average W_{ei} was 3.16 ± 0.33 gC per kg H_2O.

The correlation matrix and significance test between W_{ue}, W_{ei}, and climatic variables at the interannual scale are shown in Table 2. The only significant correlation between W_{ue} and the climatic variable is W_{ue} and precipitation (P_{recip}) during the dry season ($r = -0.66$, $p < 0.05$), whereas the interannual variation of W_{ei} could be well explained by water-related variables (V_{PD}, S_{WC}, and P_{recip}) in the dry season or at the annual scale, but not for rainy season observations (Table 2).

3.5. Controls of V_{PD} on W_{ue} at Multiscales

It has long been recognized that V_{PD} exerts a strong control over W_{ue} over short time scales [*Bierhuizen and Slatyer*, 1965]. We affirm this relationship with our instantaneous 30 min data in the eight sample days (Figure 6a) and in whole year 2003 (Figure 4b). W_{ue} was better fitted to $1/(V_{PD})^{0.5}$ ($r = 0.46$) than to $1/V_{PD}$ ($r = 0.38$). The daily binned W_{ue} was also significantly related to V_{PD} ($r = -0.38$, $p < 0.0001$). The relationship could be largely improved by removing values with V_{PD} larger than 9 hPa ($r = -0.61$) (Figure 8b). The period with $V_{PD} > 9$ hPa occurred in the late dry season (Figure 5b values above grey line), coinciding with the lowest soil water content and peak leaf shedding. No correlation has been detected between V_{PD} and W_{ue} at the interannual scale (Figure 8c).

Table 1. Correlation Coefficients and Their Significance Tests Between Biotic and Climatic Variables and Water Use Efficiency at the Annual Scale[a]

	V_{PD}	T_a	R_g	S_{WC}	L_{AI}	k_t
W_{ue}	−0.3814**	−0.5501**	−0.4182**	−0.2501**	0.3304**	0.1048*
W_{ei}	0.8701**	0.4798**	0.4744**	−0.3198**	−0.7704**	−0.0654

[a]Data for the correlation were multiyear daily mean values, with a total of 365 samples. Single and double asterisks indicate statistical significance at the 0.05 and 0.01 levels, respectively.
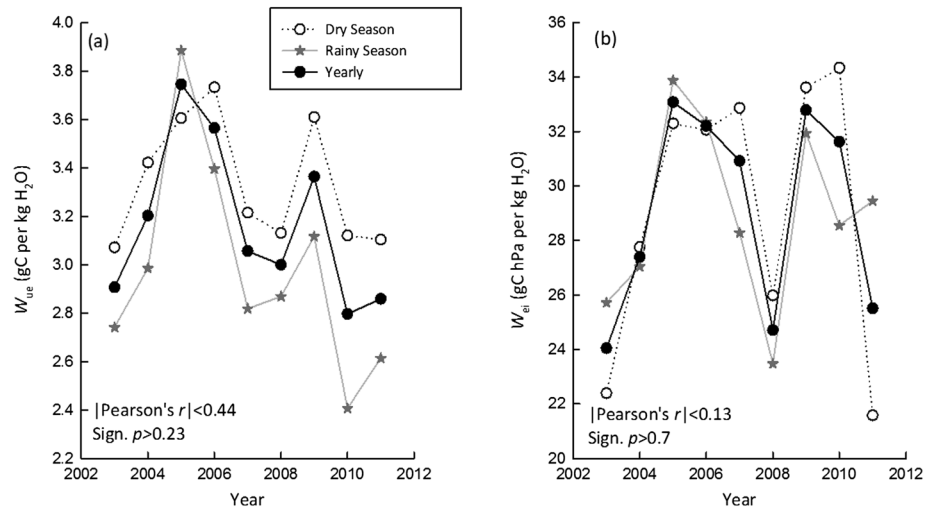
Figure 7. (a) Interannual variation of water use efficiency and (b) inherent water use efficiency annual means or seasonal means. Dry season: open circles connected by dashed line; rainy season: stars connected by grey line; annual: solid circles with black line. Sign p represents significance of Mann-Kendall test.

3.6. Response of W_{ue}, W_{ei} to Severe Regional Drought

Rainfall is strongly seasonal, with 87% of it occurring during the rainy half-year (Figure 9a). It was reported that native rainforests here utilize rainy season rainfall stored in the soil to overcome water shortage during the dry season [*Li et al.*, 2010]. Rainfall has decreased since the rainy season of 2009, and the reduced rainfall continued until the end of the dry season in 2010 (Figure 9b). This rainfall shortage or meteorological drought occurred regionally [*Qiu*, 2010]. No general response pattern of W_{ue} to the drought was detected from comparing observations during the drought period with 9 year mean values (paired t test, $p = 0.086$) (Figure 9c). W_{ue} was greatly increased in November and December during the drought. By examining G_{PP} and T_r during this period (Figures 9d and 9e), it can be seen that increased W_{ue} in November and December was caused by increased G_{PP} and decreased T_r. In the middle and late dry season (January to March), when drought was aggravated, drought G_{PP} was obviously lower than the average values. T_r was also reduced during the drought but showed more monthly variation (Figure 9e).

4. Discussion and Conclusions

4.1. Forest W_{ue}

Literature-based forest W_{ue} is summarized in Table 3. Mean W_{ue} values for boreal, temperate, subtropical, and tropical forest are 3.25 ± 0.50, 4.30 ± 1.13, 2.25 ± 0.33, and 3.16 ± 0.00 gC per kg H_2O, respectively. The W_{ue} of tropical forests is close to that of boreal forests, higher than subtropical forests, and lower than temperate forests. It is worth noting that few data on tropical forest W_{ue} were available for comparison (Table 3). Most previous studies have concentrated on temperate forests. Year-round data across seasons were used in

Table 2. Pearson's Correlation Between Annual Water Use Efficiency (W_{ue}) and Intrinsic Water Use Efficiency (W_{ei})[a]

	Dry Season		Rainy Season		Yearly	
	W_{ue}	W_{ei}	W_{ue}	W_{ei}	W_{ue}	W_{ei}
T_a	−0.0319	0.1490	−0.0987	0.1697	−0.1362	0.5114
R_g	−0.1553	−0.0967	−0.0657	0.1981	−0.1265	−0.1232
V_{PD}	0.2800	0.8917**	−0.4259	0.3375	−0.0720	0.6881*
S_{WC}	−0.5422	−0.8441**	−0.0206	−0.4353	−0.3620	−0.7287*
P_{recip}	−0.6639*	−0.6605*	0.3289	−0.2292	0.1183	−0.2352

[a]There were nine samples total. Single and double asterisks indicate statistical significant at the 0.05 and 0.01 levels, respectively.
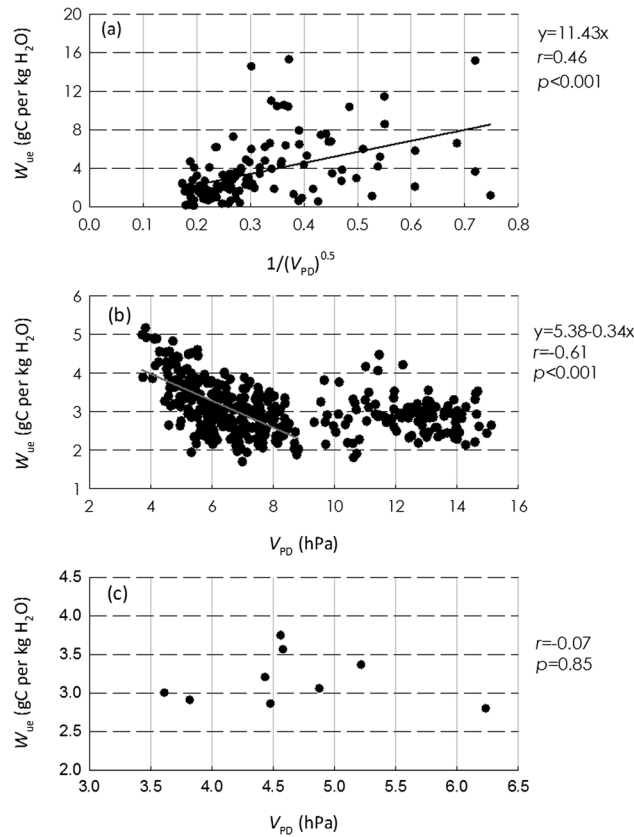
Figure 8. The control of water vapor deficit on water use efficiency at the (a) instantaneous, (b) seasonal, and (c) interannual scales. Regression line in Figure 8b is only for when V_{PD} is less than 9 hPa. The p value is two-tailed.

estimating annual W_{ue} for both subtropical and tropical forests. In contrast, only growing season data were used for W_{ue} calculation in high-latitude forests such as temperate and boreal forests. To well-utilizing resources in growing season, leaf photosynthesis in warm growing season is generally higher in deciduous than that of evergreen trees [*Givnish*, 2002]. It could be the reason for highest W_{ue} observed in temperature forests. Though tropical forests was well known for high G_{PP} [*Malhi et al.*, 1999], the high T_r lead to moderate but not highest W_{ue} in these forests.

As listed in literature review Table 3, the mean W_{ue} values for evergreen needle forest (ENF), evergreen broadleaved forest (EBF), deciduous broadleaved forest (DBF), and mixed forest (MF) are 3.55 ± 1.04, 2.83 ± 0.63, 4.85 ± 1.08, and 3.88 ± 1.25 gC per kg H_2O, respectively. This is consistent with results derived from linear regression between ET and G_{PP}, which suggests that DBF's W_{ue} is higher than that of ENF [*Law et al.*, 2002], but the estimated W_{ei} from the summary table is higher than that reported by *Law et al.* [2002] (ENF: 2.43; DBF: 3.42 gC per kg H_2O). These differences could partly be explained by the different calculation procedures. Total ET was used in *Law et al.* [2002], while only dry canopy data were used for the data summarized in Table 3. Tropical forests were categorized into EBF which has lowest W_{ue}. EBF usually existed under warm and wet climate, i.e., wet subtropical and tropical land. Forests under this climate will invest less to develop system to improve water use efficiency since water condition usually is not tough.

4.2. Interannual Trend of W_{ei}

By compiling data from 21 flux towers in temperate and boreal forests, *Keenan et al.* [2013] detected an increasing trend in W_{ei}. After removing the confounding effect of other climatic factors, they concluded that forest W_{ei} was stimulated by the increasing CO_2 concentration. We did not find an increasing W_{ei} trend in our studied tropical forest (Figure 7b). With data from only one site, it is risky to conclude that the tropical forest W_{ei} was not increased by CO_2 stimulation. Here we try to consider some other clues which might be helpful in addressing the trend in tropical forest W_{ei}:

1. *Tropical forest growth has declined in the past*. Stem growth of tropical forest trees was reported to be steadily decreasing over a 16 year period of observation at a Costa Rica rainforest [*Clark et al.*, 2003]. *Feeley et al.* [2007] confirmed this trend by analyzing 50 ha plot data from Panama and Malaysia. Using 10 year inventory data from a 1 ha plot, we also observed a decreasing growth rate in our studied rainforest [*Tan et al.*, 2013]. Although tree growth could not directly explain W_{ei} by transpiration, respiration, and allocation [*Nock et al.*, 2011], they are generally supposed to be positively correlated. For example, forests with increasing W_{ei} will have increasing carbon sink strength [*Keenan et al.*, 2013].
2. *Forest growth is linked to climatic variation but not to increasing CO_2*. The growth of Costa Rica's rainforests has been linked to climatic variations, but not to increasing CO_2 [*Clark et al.*, 2010, 2013]. *Dong et al.* [2012] found tree growth rates in four tropical forests that could be explained by solar radiation and temperature.
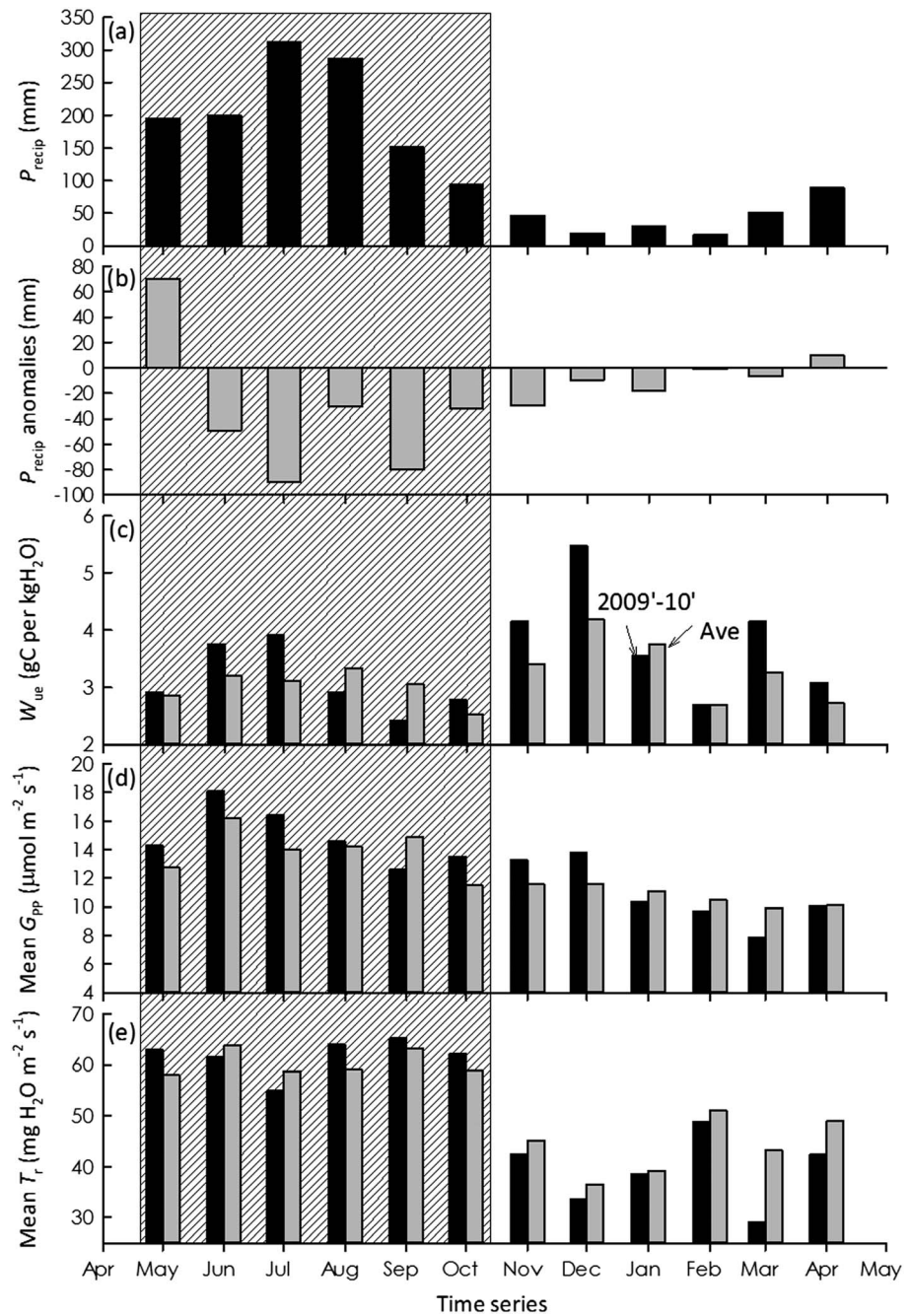
Figure 9. The impact of the 2009–2010 drought on ecosystem water use efficiency. (a) Mean precipitation in past years (1959–2011); (b) rainfall anomalies: precipitation in 2009–2010 minus mean precipitation; (c) water use efficiency; (d) gross primary production; and (e) transpiration. Black bars represent values during May 2009 to April 2010, and grey bars indicate 9 year mean values.

In our studied forest, the declining tree growth was well explained by the interannual variation of net water balance [*Tan et al.*, 2013]. That is to say, CO_2's stimulating effect on W_{ei} might be small when compared with the effect of climatic perturbations.

3. W_{ei} *was correlated to interannual climatic variations*. The interannual dynamics of W_{ei} were correlated significantly with water conditions, especially during the dry season (V_{PD}, S_{WC}, and P_{recip}) (Table 2). P_{recip} was the primary determinant of the interannual variations of W_{ei} ($r = 0.96$), with the exception of years 2009 and 2010, when there was a severe drought (Figure 10). The high W_{ei} retained during the severe drought might be the result of high V_{PD} during that period.

Table 3. Literature-Based Forest W_{ue}[a]

Forest Zone[a]	Site	IGBP	Rainfall (mm)	Temperature (°C)	Stand Age (Year)	W_{ue} (gC per kg H2O)	References
Boreal	Howland, USA	ENF	988	6.1	100	3.98	(1), (2)
	Saskatchewan, Canada	ENF	467	0.4	87	3.41	(2), (3)
	Saskatchewan, Canada	ENF	467	0.4	130	3.05	(2), (4)
	Flakaliden, Sweden	ENF	105	4.3	43	2.66	(2), (5)
	Hyytiälä, Finland	ENF	709	2.9	40	3.61	(2), (6)
	Sodankylä, Finland	ENF	499	−1.0	100	2.82	(2), (7)
Temperate	Changbaishan, China	MF	695	3.6	200	2.57	(8)
	Collelongo, Italy	DBF	1100	7.2	90	6.07	(2), (9)
	Vancouver, USA	ENF	1451	8.6	55	5.4	(10)
	Thuringia, Germany	ENF	1944	6.6	50	5.42	(2), (11)
	Vielsalm, Belgium	MF	1000	7	60	5.08	(2), (12)
	Le Bray, France	ENF	1860	15	28	2.63	(2), (13)
	De Inslag, Belgium	MF	750	9.8	70	3.99	(2), (14)
	Loobos, Netherlands	ENF	786	9.8	100	3.77	(2), (15)
	Hesse, France	DBF	820	9.2	30	4.51	(2), (16)
	Tharandt, Germany	ENF	823	7.8	120	4.55	(2), (17)
	Hainich, Germany	DBF	780	7.8	250	5.31	(2), (18)
	Puéchabon, France	EBF	883	13.5	60	3.14	(2), (19)
	Viterbo, Italy	DBF	755	14	20	3.54	(2), (20)
Subtropical	Qianyanzhou, China	ENF	1485	17.9	21	2.52	(8)
	Dinghushan, China	EBF	1956	21	100	1.88	(8)
Tropical	Florida, USA	ENF	1332	20	10	2.35	(2), (21)
	Espiritu Santo, Vanuatu	EBF	2763	24.5	22	3.17	(2), (22)
	Xishuangbanna, China	EBF	1500	21.5	200	3.16	(23)

[a]Forest zone was determined by considering species composition, geographic location, and Whittaker biome diagram. IGBP represents International Geosphere-Biosphere Program. ENF, EBF, DBF, and MF represent evergreen needle forest, evergreen broadleaved forest, deciduous broadleaved forest, and mixed forest, respectively. (1): *Hollinger et al.* [1999], (2): *Beer et al.* [2009], (3): *Krishnan et al.* [2006], (4): *Krishnan et al.* [2008], (5): *Lindroth et al.* [2008], (6): *Suni et al.* [2003], (7): *Thum et al.* [2007], (8): *Yu et al.* [2008], (9): *Valentini et al.* [1996], (10): *Ponton et al.* [2006], (11): *Anthoni et al.* [2004], (12): *Aubinet et al.* [2002], (13): *Berbigier et al.* [2001], (14): *Carrara et al.* [2004], (15): *Dolman et al.* [2002], (16): *Granier et al.* [2000], (17): *Grünwald and Bernhofer* [2007], (18): *Knohl et al.* [2003], (19): *Rambal et al.* [2003], (20): *Tedeschi et al.* [2006], (21): *Clark et al.* [2004], (22): *Roupsard et al.* [2006], and (23): this study.

4.3. Controls on W_{ue} at Different Scales

Plant water use efficiency has been reported to be controlled by a series of variables, including CO_2 levels [*Keenan et al.*, 2013], leaf area index [*Beer et al.*, 2009], water vapor pressure deficit [*Yang et al.*, 2010], and sky clearness [*Rocha et al.*, 2004]. The controls vary among sites and across scales. In our site data, for example, V_{PD} exerts a strong control on instantaneous or seasonal W_{ue}, but not on the interannual variations (Figure 8). The strong control of V_{PD} on instantaneous W_{ue} has been well documented and widely tested [*Yang et al.*, 2010]. We must state here that our data support the prediction of stomatal optimization theory on this control [*Katul et al.*, 2009], which is indicated by the fact that W_{ue} was better fitted to $1/(V_{PD})^{0.5}$ ($r = 0.46$) than $1/V_{PD}$ ($r = 0.38$). Few attempts have been made to investigate V_{PD}'s control of W_{ue} at the seasonal scale. *Jassal et al.* [2009] reported that W_{ue} decreased with V_{PD} at the seasonal scale in a Douglas fir stand, and the negative relationship is mainly based on wintertime observations (November–February). If data from the winter period were removed, the relationship would become very weak. We found similar results in our data set. If data from DOY 1–30 and 330–365 were removed, the correlation becomes very weak ($r = -0.12$, slope $= -0.02$, $p = 0.04$). In addition, W_{ue} during the high V_{PD} period ($V_{PD} > 9$ hPa) is not sensitive to change in V_{PD} at our site (Figure 8). To our knowledge, our study is the first report on how V_{PD} controls the interannual ecosystem W_{ue}. We did not find significant seasonal or annual correlations between interannual V_{PD} and W_{ei} (Figure 8).

Temperature is the leading control on the seasonal variation of W_{ue} (Figure 6), and the two factors are negatively correlated ($r = -0.55$). This relationship is similar to that found in a Chinese subtropical forest, but contrary to that found in temperate forests [*Zhu et al.*, 2014]. The L_{Al} increased with temperature and had a strong impact on W_{ue}. This was used to explain the positive correlation found in temperate forests by *Zhu et al.* [2014], who attributed the negative correlation between temperature and W_{ue} found in subtropical forests to soil water stress. This was not the case in our study. The correlation of W_{ue} to S_{WC} is weaker than to T_a (Table 1). According to the water stress explanation, S_{WC} but not T_a is the dominant driving force of seasonal W_{ue}. A possible explanation for the negative correlation between T_a and W_{ue} could be continuous, relatively high photosynthesis during low-temperature periods. G_{PP} decreased during low-temperature periods, but the decrease is less than that of T_r (Figure 9d, 9 year average).
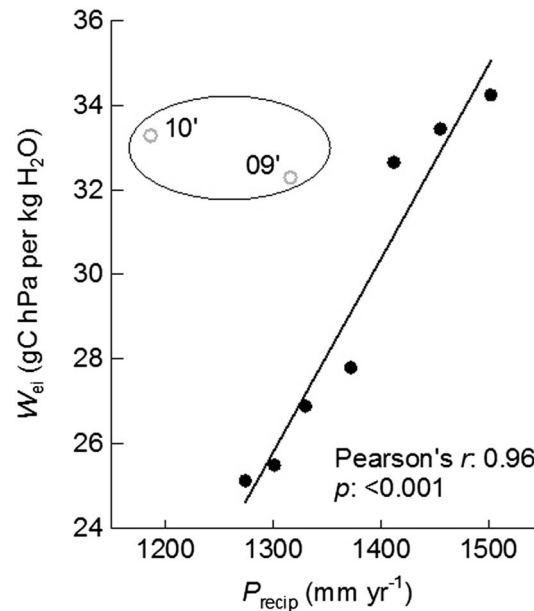
Figure 10. Relationship between annual precipitation (P_{recip}) and inherent water use efficiency (W_{ei}). Data from 2009 and 2010 when a drought occurred were not included in the linear regression. The p value is two-tailed.

Continuous and relatively high photosynthesis rates have also been reported in subtropical evergreen broadleaved forests [*Tan et al.*, 2012]. The annual temperature range in our study site is ~10°C, which is similar to southern subtropical sites, such as Dinghushan in Guangzhou [*Tan et al.*, 2012]. Continuous high photosynthesis might be a common property for evergreen forests near the Tropic of Cancer. In contrast, T_r is more sensitive to decreasing temperature than G_{PP}, as shown in our data (Figure 9e) and as derived from the Penman-Monteith principles.

4.4. Response of W_{ue} to Drought

The response of W_{ue} to drought is a much debated topic [*Wolf et al.*, 2013]. What is known about leaf stomata predicts an increase of W_{ue} during droughts by continuous high levels of photosynthesis [*Schulze*, 2006]. *There was no significant difference between* W_{ue} *during the drought and the 9 year mean values in our studied forest* (Figure 9c), but we found that the dry season T_r was consistently lower than the mean values during the drought (Figure 9f). This supports the idea that T_r decreases during a drought [*Jarvis and McNaughton*, 1986]. Reduced T_r during a drought was also reported in a European forest using stored water in deep soil [*Teuling et al.*, 2010]. Declining T_r could lead to increasing W_{ue} if photosynthesis levels remain high during a drought, as was found for a mixed and evergreen needle forest in Switzerland [*Wolf et al.*, 2013] and a boreal forest in Canada [*Krishnan et al.*, 2006]. In some cases, there was a larger decline in G_{PP} than in T_r during a drought, resulting in decreased W_{ue} [*Reichstein et al.*, 2007]. In the case of tropical forests, it is much more complicated. *Malhi et al.* [2002] found that limited water availability during the dry season caused evapotranspiration to reduce by 50%. Studies in a per humid Bonean rainforest showed that transpiration was positively correlated to V_{PD} [*Kume et al.*, 2011]. The water seasonality is strong in our study site. Drought reduced water availability and subsequently leads to reduction in T_r even though V_{PD} is high the period. The response of an ecosystem's W_{ue} to drought is still an open question, and more studies are needed to establish the common principles that govern it.

References

Anthoni, P. M., A. Knohl, C. Rebmann, A. Freibauer, M. Mund, W. Ziegler, O. Kolle, and E.-D. Schulze (2004), Forest and agricultural land-use-dependent CO_2 exchange in Thuringia, Germany, *Global Change Biol.*, 10, 2005–2019.

Aubinet, M., B. Heinesch, and B. Longdoz (2002), Estimation of the carbon sequestration by a heterogeneous forest: Night flux corrections, heterogeneity of the site and inter-annual variability, *Global Change Biol.*, 8, 1053–1071.

Aubinet, M., C. Feigenwinter, B. Heinesch, C. Bernhofer, E. Canepa, A. Lindroth, L. Montagnani, C. Rebmann, P. Sedlak, and E. Van Gorsei (2010), Direct advection measurements do not help to solve the nighttime CO_2 closure problem: Evidence from three different forests, *Agric. For. Meteorol.*, 150, 655–664.

Baldocchi, D. (1994), A comparative study of mass and energy exchange rates over a closed C3 (wheat) and an open C4 (corn) crop: II. CO_2 exchange and water use efficiency, *Agric. For. Meteorol.*, 67, 291–321.

Baldocchi, D. D., B. B. Hincks, and T. P. Meyers (1988), Measuring biosphere-atmosphere exchanges of biologically related gases with micrometeorological methods, *Ecology*, 69, 1331–1340.

Beer, C., M. Reichstein, P. Ciais, G. D. Farquhar, and D. Papale (2007), Mean annual GPP of Europe derived from its water balance, *Geophys. Res. Lett.*, 34, L05401, doi:10.1029/2006GL029006.

Beer, C., et al. (2009), Temporal and among-site variability of inherent water use efficiency at the ecosystem level, *Global Biogeochem. Cycles*, 23, GB2018, doi:10.1029/2008GB003233.

Berbigier, P., J.-M. Bonnefond, and P. Mellmann (2001), CO_2 and water vapor fluxes for 2 years above Euroflux forest site, *Agric. For. Meteorol.*, 108, 183–197.

Bierhuizen, J. F., and R. O. Slatyer (1965), Effects if atmospheric concentration of water vapor and CO_2 in determining transpiration-photosynthesis relationships of cotton leaves, *Agric. Meteorol.*, 2, 259–270.

Burba, G. (2013), *Eddy Covariance Method for Scientific, Industrial, Agricultural and Regulatory Applications: A Field Book on Measuring Ecosystem Gas Exchanges and Areal Emission Rates*, 331 pp., Li-Cor Biosciences, Lincoln.

Carrara, A., I. A. Janssens, J. C. Yuste, et al. (2004), Seasonal changes in photosynthesis, respiration and NEE of a mixed temperate forest, *Agric. For. Meteorol.*, *126*, 15–31.

Clark, D. A., S. C. Piper, C. D. Keeling, and D. B. Clark (2003), Tropical rain forest tree growth and atmospheric carbon dynamics linked to interannual temperature variation during 1984–2000, *Proc. Natl. Acad. Sci. U.S.A.*, *100*, 5852–5857.

Clark, D. A., D. B. Clark, and S. F. Oberbauer (2013), Field-quantified responses of tropical rainforest aboveground productivity to increasing CO_2 and climatic stress, 1997–2009, *J. Geophys. Res. Biogeosci.*, *118*, 783–794, doi:10.1002/jgrg.20067.

Clark, D. B., D. A. Clark, and S. F. Oberbauer (2010), Annual wood production in a tropical rain forest in NE Costa Rica linked to climatic variation but not to increasing CO_2, *Global Change Biol.*, *16*, 747–759.

Clark, K. L., H. L. Gholz, and M. S. Castro (2004), Carbon dynamics along a chronosequence of slash pine plantations in north Florida, *Ecol. Appl.*, *14*, 1154–1171.

Cowan, I. R., and G. D. Farquhar (1977), Stomatal function in relation to leaf metabolism and environment, in *Integration of Activity in the Higher Plant*, edited by D. H. Jennings, pp. 471–505, Cambridge Univ. Press, Cambridge, U. K.

deWit, C. T. (1958), Transpiration and crop yield, Institute of Biological and Chemical Research on Field Crops and Herbage.

Dolman, A. J., E. J. Moors, and J. A. Elbers (2002), The carbon uptake of a mid latitude pine forest growing on sandy soil, *Agric. For. Meteorol.*, *111*, 157–170.

Dong, X., S. J. Davies, P. S. Ashton, S. Bunyavejchewin, M. N. Nur Supardi, A. R. Kassim, S. Tan, and P. R. Moorcroft (2012), Variability in solar radiation and temperature explains observed patterns and trends in tree growth rates across four tropical forests, *Proc. R. Soc. B*, *279*, 3923–3931.

Falge, E., et al. (2001), Gap fillings strategies for defensible annual sums of net ecosystem exchange, *Agric. For. Meteorol.*, *107*, 43–69.

Feeley, K. J., S. J. Wright, M. N. N. Supardi, A. R. Kassim, and S. J. Davies (2007), Decelerating growth in tropical forest trees, *Ecol. Lett.*, *10*, 461–469.

Givnish, T. J. (2002), Adaptive significance of evergreen vs. deciduous leaves: Solving the triple paradox, *Silva Fennica*, *36*, 703–743.

Goulden, M. L., J. W. Munger, S.-M. Fan, B. C. Daube, and S. C. Wofsy (1996), Measurements of carbon sequestration by long-term eddy covariance: Methods and a critical evaluation of accuracy, *Global Change Biol.*, *2*, 169–182.

Granier, A., et al. (2000), The carbon balance of a young beech forest, *Funct. Ecol.*, *14*, 312–325.

Grünwald, T., and C. Bernhofer (2007), A decade of carbon, water and energy flux measurements of an old spruce forest at the Anchor Station Tharandt, *Tellus*, *59B*, 387–396.

Gu, L., J. Fuentes, and H. Shugart (1999), Response of net ecosystem exchange of carbon dioxide to changes in cloudiness: Results from two North American deciduous forests, *J. Geophys. Res.*, *104*, 31,421–31,434, doi:10.1029/1999JD901068.

Hollinger, D. Y., F. M. Kelliher, J. N. Byers, J. E. Hunt, T. M. McSeveny, and P. L. Weir (1994), Carbon dioxide exchange between an undisturbed old-growth temperate forest and the atmosphere, *Ecology*, *75*, 134–150.

Hollinger, D. Y., S. M. Goltz, E. A. Davidson, J. T. Lee, K. Tu, and H. T. Valentine (1999), Seasonal patterns and environmental control of carbon dioxide and water vapor exchange in an ecotonal boreal forest, *Global Change Biol.*, *5*, 891–902.

Hsiao, T. C., and E. Acevedo (1974), Plant responses to water deficits, water-use efficiency and drought resistance, *Agric. Meteorol.*, *14*, 59–84.

Jarvis, P. G., and K. G. McNaughton (1986), Stomatal control of transpiration: Scaling up from leaf to region, *Adv. Ecol. Res.*, *15*, 1–49.

Jassal, R. S., T. A. Black, D. L. Spittlehouse, C. Brümmer, and Z. Nesic (2009), Evapotranspiration and water use efficiency in different-aged Pacific Northwest Douglas-fir stands, *Agric. For. Meteorol.*, *149*, 1168–1178.

Katul, G. G., S. Palmroth, and R. Oren (2009), Leaf stomatal responses to vapor pressure deficit under current and CO_2-riched atmosphere explained by the economics of gas exchange, *Plant, Cell Environ.*, *32*, 968–979.

Keenan, T. F., D. Y. Hollinger, G. Bohrer, D. Dragoni, J. W. Munger, H. P. Schmid, and A. D. Richardson (2013), Increase in forest water-use efficiency as atmospheric carbon dioxide concentrations rise, *Nature*, *499*, 324–327.

Knohl, A., E.-D. Schulze, O. Kolle, and N. Buchmann (2003), Large carbon uptake by an unmanaged 250-year-old deciduous forest in Central Germany, *Agric. For. Meteorol.*, *118*, 151–167.

Krishnan, P., T. A. Black, N. J. Grant, A. G. Barr, E. H. Hogg, R. S. Jassal, and K. Morgenstern (2006), Impact of changing soil moisture distribution on net ecosystem productivity of a boreal aspen forest during and following drought, *Agric. For. Meteorol.*, *139*, 208–223.

Krishnan, P., T. A. Black, A. G. Barr, N. J. Grant, D. Gaumont-Guay, and Z. Nesic (2008), Factors controlling the interannual variability in the carbon balance of a southern boreal black spruce forest, *J. Geophys. Res.*, *113*, D09109, doi:10.1029/2007JD008965.

Kume, T., N. Tanaka, K. Kuraji, H. Komatsu, N. Yoshifuji, T. M. Saitoh, M. Suzuki, and T. Kumagai (2011), Ten-year evapotranspiration estimates in a Bornean tropical rainforest, *Agric. For. Meteorol.*, *151*, 1183–1192.

Lange, O. L., R. Losch, E. D. Schulze, and L. Kappen (1971), Response of stomata to changes in humidity, *Planta*, *100*, 76–86.

Law, B. E., et al. (2002), Environmental controls over carbon dioxide and water vapor exchange of terrestrial vegetation, *Agric. For. Meteorol.*, *113*, 97–120.

Li, Z., Y. Zhang, S. Wang, G. Yuan, Y. Yang, and M. Cao (2010), Evapotranspiration of a tropical rain forest in Xishuangbanna, southwest China, *Hydrol. Processes*, *24*, 2405–2416.

Lin, H., M. Cao, and Y. Zhang (2011), Self-organization of tropical seasonal rain forest in southwest China, *Ecol. Modell.*, *222*, 2812–2816.

Linares, J. C., and J. J. Camarero (2012), From pattern to process: Linking intrinsic water-use efficiency to drought-induced forest decline, *Global Change Biol.*, *18*, 1000–1015.

Lindroth, A., L. Klemedtsson, A. Grelle, P. Weslien, and O. Langvall (2008), Measurement of net ecosystem exchange, productivity and respiration in three spruce forests in Sweden shows unexpectedly large soil carbon losses, *Biogeochemistry*, *89*, 43–60.

Lloyd, J., and J. A. Taylor (1994), On the temperature dependence of soil respiration, *Funct. Ecol.*, *8*, 315–323.

Malhi, Y., D. D. Baldocchi, and P. G. Jarvis (1999), The carbon balance of tropical, temperate and boreal forests, *Plant Cell Environ.*, *22*, 715–740.

Malhi, Y., E. Pegorara, A. D. Nobre, M. G. P. Pereire, J. Grace, A. D. Culf, and R. Clement (2002), Energy and water dynamics of a central Amazonian rain forest, *J. Geophys. Res.*, *107*(D20), 8061, doi:10.1029/2001JD000623.

Mencuccini, M., J. Grace, J. Moncrieff, and K. G. McNaughton (2004), *Forest at the Land-Atmosphere Interface*, CABI Publishing, Wallingford, Oxfordshire, U. K.

Monteith, J. L. (1964), Evaporation and environment, *Symp. Soc. Exp. Biol.*, *19*, 205–355.

Morén, A.-S., A. Lindroth, and A. Grelle (2001), Water-use efficiency as a means of modeling net assimilation in boreal forests, *Trees*, *15*, 67–74.

Nock, C. A., P. J. Baker, W. Wanek, A. Leis, M. Grabneg, S. Bunyavejchewin, and P. Hietz (2011), Long-term increases in intrinsic water-use efficiency do not lead to increased stem growth in a tropical monsoon forest in Thailand, *Global Change Biol.*, *17*, 1049–1063.

Pan, Y. D., et al. (2011), A large and persistent carbon sink in the world's forests, *Science*, *333*, 988–993.

Peñuelas, J., J. G. Canadell, and R. Ogaya (2011), Increase water-use efficiency during the 20th century did not translate into enhanced tree growth, *Global Ecology Biogeogr.*, *20*, 597–608.

Ponton, S., L. B. Flanagan, K. P. Alstad, B. G. Johnson, K. Morgenstern, N. Kljun, T. A. Black, and A. G. Barr (2006), Comparison of ecosystem water-use efficiency among Douglas-fir forest, aspen forest and grassland using eddy covariance and carbon isotope techniques, *Global Change Biol.*, *12*, 294–310.

Qiu, J. (2010), China drought highlights future climate threats, *Nature*, *465*, 142–143.

Rambal, S., J.-M. Ourcival, R. Joffre, F. Mouillot, Y. Nouvellon, M. Reichstein, and A. Rocheteau (2003), Drought controls over conductance and assimilation of a Mediterranean evergreen ecosystems: Scaling from leaf to canopy, *Global Change Biol.*, *9*, 1813–1824.

Reichstein, M., et al. (2005), On the separation of net ecosystem exchange into assimilation and ecosystem respiration: Review and improved algorithm, *Global Change Biol.*, *11*, 1424–1439.

Reichstein, M., et al. (2007), Reduction of ecosystem productivity and respiration during the European summer 2003 climate anomaly: A joint flux tower, remote sensing and modelling analysis, *Global Change Biol.*, *13*, 634–651.

Rocha, A. V., H. B. Su, C. A. Vogel, H. P. Schmid, and P. S. Curtis (2004), Photosynthetic and water use efficiency responses to diffuse radiation by an aspen-dominated northern hardwood forest, *For. Sci.*, *50*, 793–801.

Roupsard, O., et al. (2006), Partitioning energy and evapo-transpiration above and below a tropical palm canopy, *Agric. For. Meteorol.*, *139*, 252–268.

Schulze, E.-D. (2006), Biological control of the terrestrial carbon sink, *Biogeosciences*, *3*, 147–166.

Sinclair, T. R., C. B. Tanner, and J. M. Bennett (1983), Water-use efficiency in crop production, *BioScience*, *34*, 36–40.

Suni, T., J. Rinne, A. Reissell, N. Altimir, P. Keronen, Ü. Rannik, M. Dal Maso, M. Kulmala, and T. Vesala (2003), Long-term measurements of surface fluxes above a Scots pine forest in Hyytiälä, southern Finland, 1996–2001, *Boreal Environ. Res.*, *8*, 287–301.

Swinbank, W. C. (1951), The measurement of vertical transfer of heat and water vapor by eddies in the lower atmosphere, *J. Meteorol.*, *8*, 135–145.

Tan, Z., Y. Zhang, G. Yu, Q. Song, Z. Yang, J. Gao, M. Zhang, and N. Liang (2009), Ecosystem physiological properties of a primary tropical seasonal rainforest, 1, temporal pattern of fluxes and its environmental responses, paper presented in the 26th Annual Meeting of Chinese Meteorological Society, Beijing.

Tan, Z., Y. Zhang, Q. Song, G. Yu, and N. Liang (2014), Leaf shedding as an adaptive strategy for water deficit: A case study in Xishuangbanna's rainforest, *J. Yunnan Univ.*, *36*, 273–280.

Tan, Z.-H., et al. (2012), An observational study of the carbon sink strength of East Asian subtropical evergreen forests, *Environ. Res. Lett.*, *7*, 044017, doi:10.1088/1748-9326/7/4/044017.

Tan, Z.-H., et al. (2013), High sensitivity of a tropical rainforest to water variability: Evidence from 10 years of inventory and eddy flux data, *J. Geophys. Res. Atmospheres*, *118*, 9393–9400, doi:10.1002/jgrd.50675.

Tedeschi, V., A. Rey, G. Manca, R. Valentini, P. G. Jarvis, and M. Borghetti (2006), Soil respiration in a Mediterranean oak forest at different developmental stages after copping, *Global Change Biology*, *12*, 110–121.

Teuling, A. J., et al. (2010), Contrasting response of European forest and grassland energy exchange to heatwaves, *Nat. Geosci.*, *3*, 722–727.

Thum, T., T. Aalto, T. Laurila, M. Aurela, P. Kolari, and P. Hari (2007), Parameterization of two photosynthesis models at the canopy scale in a northern boreal Scots pine forest, *Tellus*, *59B*, 874–890.

Valentini, R., P. De Angelis, G. Matteucci, R. Monaco, S. Dore, and G. E. Scarascia Mucnozza (1996), Seasonal net carbon dioxide exchange of a beech forest with the atmosphere, *Global Change Biol.*, *2*, 199–207.

Wolf, S., W. Eugster, C. Ammann, M. Hani, S. Zielis, R. Hiller, J. Stieger, D. Imer, L. Merhold, and N. Buchmann (2013), Contrasting response of grassland versus forest carbon and water fluxes to spring drought in Switzerland, *Environ. Res. Lett.*, *8*, 035007, doi:10.1088/1748-9326/8/3/035007.

Xiao, J. F., et al. (2013), Carbon fluxes, evapotranspiration, and water use efficiency of terrestrial ecosystems in China, *Agric. For. Meteorol.*, *182*(183), 76–90.

Yang, B., et al. (2010), Environmental controls on water use efficiency during severe drought in an Ozark forest in Missouri, USA, *Global Change Biol.*, *16*, 2252–2271.

Yu, G., X. Song, Q. Wang, Y. Liu, D. Guan, J. Yan, X. Sun, L. Zhang, and X. Wen (2008), Water-use efficiency of forest ecosystems in eastern China and its relations to climatic variables, *New Phytol.*, *177*, 927–937.

Zhang, Y., Z. Tan, Q. Song, G. Yu, and X. Sun (2010), Respiration controls the unexpected seasonal pattern of carbon flux in an Asian tropical rain forest, *Atmos. Environ.*, *44*, 3886–3893.

Zhu, H., and L. Yan (2009), Biogeographical affinities of the flora of southeastern Yunnan China, *Botanical Stud.*, *50*, 467–475.

Zhu, X., G. Yu, Q. Wang, Z. Hu, S. Han, J. Yan, Y. Wang, and L. Zhao (2014), Seasonal dynamics of water use efficiency of typical forest and grassland ecosystems in China, *J. For. Res.*, *19*, 70–76.